Surface Tensions in NaCl−Water−Air Systems from MD Simulations

Ranjit Bahadur,[†] Lynn M. Russell,*[,†] and Saman Alavi[‡]

Scripps Institution of Oceanography, University of California San Diego, La Jolla, California 92093-0221, and Steacie Institute for Molecular Sciences, National Research Council of Canada, Ottawa, Ontario K1A 0R6, Canada

Received: July 9, 2007; In Final Form: July 30, 2007

Surface tensions for liquid−vapor (lv), solid−liquid (sl), and solid−vapor (sv) interfaces are calculated from molecular dynamics simulations of the NaCl−water−air system. Three distinct calculation techniques based on thermodynamic properties are used to describe the multicomponent mixtures. Simulations of each bulk phase (including a liquid saturated solution) and various interfaces are carried out at both NPT and NVT conditions. The thermodynamic relation for energy difference between interface and bulk phases provides an upper bound to the surface tension, while the energy-integral and test area methods provide direct estimates. At 1 atm and 300 K, the best predictions for surface tensions are σ^{sv} (NaCl−air) of 114 mN m^{-1}, σ^{sl} (NaCl−soln) of 63 mN m^{-1}, σ^{lv} (soln−air) of 82 mN m^{-1}, and σ^{lv} (water−air) of 66 mN m^{-1}. The calculated surface tensions from simulations have uncertainties between 5 and 10%, which are higher than measurements for the liquid interfaces and lower than the measurement uncertainty for the solid interfaces. The calculated upper bounds for surface tensions of liquid interfaces compare well with experimental results but provide no improvement over existing measurements. However, the bounding values for solid interfaces lower uncertainty by as much as a factor of 10 as compared to the indirect experimental measurements currently available. The energy-integral and test area methods appear to underestimate the surface tension of water by 10%, which is consistent with previous studies using similar model potentials. The calculated upper bounds of surface tension show a weakly positive correlation with pressure in the 0.1−100 atm range for liquid−solid, liquid−vapor, and solid−vapor interfaces.

I. Introduction

Interfacial systems are widespread in nature and industry.[1] Interfaces between water and air and among components in atmospheric aerosol, including NaCl, play an important role in atmospheric chemistry.[2−4] The surface energy of such interfaces plays a major role in water condensation and subsequent surface or aqueous phase reactions.[5,6]

Although measurements of liquid surface tensions (in contact with air, or even vacuum) are possible, there is no experimental technique to measure directly surface tensions of solids in contact with vapors or liquids due to the relative nondeformability of the solid.[7,8] Surface tension values for solids must therefore be indirectly inferred from measurements of related surface-driven phenomena using theoretical models. Additionally, such measurements that include solubility kinetics and crystallization rates have severe experimental uncertainties.[9−11] Molecular simulation techniques provide a convenient methodology to study directly the interfacial profile between two coexisting fluids or between a fluid and an adjacent solid surface.[12−16] Sodium chloride solutions as well as the crystalline phase have been widely studied using simulation techniques.[17−21] In addition to simulation of bulk phases, the dissolution properties of single ions in small water clusters have also been studied.[22,23] Recent research has focused on the interface of solid NaCl and water[24,25] and on NaCl in contact with a supersaturated solution.[26]

Computational work using both molecular dynamics (MD) and Monte Carlo (MC) techniques has focused on studying the effect of number of particles, the range of molecular interaction, and the details of simulation setup for determining the surface tension. Surface tensions calculated using various idealized potentials, system geometry, and corrections for long range interactions show good agreement with calculated results.[27−29] This study incorporates several of these well-developed simulation techniques to calculate surface tensions in three-phase systems represented by NaCl, water, and air.

II. Method and Calculations

Three general computational approaches have been used to determine the surface tension. The first, and most widespread, approach involves a mechanical route that requires the calculation of the tensorial components of the pressure. For a planar interface assumed to be perpendicular to the *z* axis of a Cartesian frame of reference, the surface tension is given by

$$\sigma = \int_{-\infty}^{\infty} (P_N(z) - P_T(z))\, dz \qquad (1)$$

where P_N and P_T are the normal and tangential components of the pressure. This mechanical expression involves the computation of the components of the pressure tensor as a function of the distance from the interface. The tensorial components can be related to the derivative of the intermolecular potential to give an explicit expression for the surface tension. The major difficulty in using the mechanical relation arises from problems in calculating components of the pressure tensor for discontinuous and truncated potentials and from applications to spherical molecules.[30]

* E-mail: lmrussell@ucsd.edu.
† University of California San Diego.
‡ National Research Council of Canada.

10.1021/jp075356c CCC: $37.00
Published on Web 09/26/2007

The second approach is based on finite-size scaling. In the case of the method developed by Binder,[31] one estimates a Landau free-energy barrier between coexisting phases from a simulation of the density of states, which in the limit of large system sizes can be related to the surface tension. This method is extremely demanding computationally and gives poor results at low temperatures due to inadequate sampling of the high-density stages.

The third approach to calculating the surface tension includes several thermodynamic or energy-based methods, in which the work of formation of an interface is used to estimate the surface tension. The standard thermodynamic relation for the Helmholtz free energy for a system containing an interface in terms of surface area A, volume V, and number of molecules N_j of each species j is[12]

$$F = -PV + \sum_j \mu_j N_j + \sigma_i A \tag{2}$$

where P is the pressure, μ_j is the chemical potential of component j, and $\sigma_i A$ is the reversible work of formation of the interface. For a system with two coexisting phases, α and β, at chemical equilibrium and the same temperature and pressure, it is possible to choose the interface to be at a dividing surface such that the difference in free energy is equal to the work of formation of the interface, that is, $\Delta\sum_j \mu_j N_j = 0$. The surface tension is then defined as the surface free energy per unit area,

$$\sigma = \frac{F^{\alpha\beta} - (F^{\alpha} + F^{\beta})}{A} \tag{3}$$

Although this relation involves three sets of simulations (one of each of the homogeneous phases and one containing a flat interface), it is simple to employ for multiple interfaces between a finite set of phases, since single-phase energies are reused. The primary advantage of this energy-based method is the easy extension to system geometries more complex than planar interfaces.

An alternate thermodynamic approach uses test areas and has the added advantage of requiring simulations only of the interface and not of either bulk phase. Small perturbations to the surface area of the interface are introduced, keeping all other properties constant. The change in free energy due to the perturbation is determined using statistical mechanical averages over the ensemble, leading to the surface tension. Gloor et al.[1] implemented this method using standard Monte Carlo techniques with idealized square well and Lennard-Jones potentials, producing accurate results at low computational costs.

In this work, we use three different thermodynamic approaches to calculate surface tensions in the NaCl−water−air system. Section 2B describes the energy difference method, which is simplest to implement, has low computational costs, and calculates upper bounds to the surface tension with limited but valuable accuracy. Section 2C presents the energy integral method described by Laird and Davidchak[29] to get direct estimates of surface tension. The method is computationally intensive but highly accurate. The test area method[1] is adapted in Section 2D using MD and compound specific potentials. The method is both relatively inexpensive computationally and accurate, although its precision for MD may be limited to about ±10%. The interfaces of interest exist between combinations of one solid (NaCl), two liquid (pure water and saturated NaCl solution), and one vapor (dry air). Since water and NaCl solution are miscible at all conditions, we exclude a liquid−liquid interface. Pure NaCl is soluble in water at all conditions,[32] and we include the NaCl−water interface as a hypothetical reference case. Table 6 summarizes calculated and measured surface tension for the five interfaces.

A. Molecular Dynamics Simulations. MD simulations were performed with the DL_POLY version 2.14[33] software using a fixed number of particles at constant temperature. The constant volume (NVT) ensemble was used in Sections 2C and 2D to calculate surface tension, and the constant pressure (NPT) ensemble was used in Section 2B to determine the pressure dependence of surface tension. Simulation cells were cubic and replicated using periodic boundary conditions and contain a number of molecules determined from bulk density. The temperature and pressure (where applicable) were held constant using the Nosé−Hoover algorithm,[34−36] with relaxation times of 0.1 and 2.0 ps used for the thermostat and barostat, respectively. The equations of motion were integrated using the Verlet leapfrog scheme.[37−39] All interatomic interactions in the simulation box were calculated within a cutoff distance of 10Å, and the Coulombic long-range interactions were calculated using Ewald's method[37−40] with a precision of 1×10^{-6}. Simulations were performed using time steps of 0.75 fs with the system being allowed to equilibrate for 100 000 steps (25 ps). Thermodynamic properties of the resulting mixture were then calculated and recorded after every 5000 simulation steps.

Ion−ion interactions in the simulations are modeled using a Born−Huggins−Mayer (BHM) potential,[41]

$$V(r_{ij}) = \frac{e^2 q_i q_j}{r_{ij}} + A_{ij}\exp(-r_{ij}/\rho_{ij}) - \frac{C_{ij}}{r_{ij}^6} - \frac{D_{ij}}{r_{ij}^8} \tag{4}$$

where V is the interaction potential, r_{ij} is the separation between ions i and j, eq_i and eq_j are the scaled atomic charges, and A_{ij}, ρ_{ij}, C_{ij}, and D_{ij} are parameters specific to each ion pair interaction. The form of the potential as written contains both attractive and repulsive terms. The potential includes both electrostatic and Lennard-Jones (LJ)-type interactions and has been shown to reproduce bulk and surface properties of simple ions.[16,42,43]

MD studies of water properties show that commonly used three- and four-point potentials replicate bulk properties such as density, structure, and self-diffusion coefficient within 5% of their measured values.[44,45] Although model potentials are also successful in replicating ion concentration profiles of water solutions even at the surface,[20,23] actual surface tension calculations have tended to under-predict values by as much as 15%.[15,46] This work includes two primary improvements over previous calculations: (1) The vapor phase is modeled as saturated air, and (2) a significantly larger interfacial cross section is used to better simulate the bulk. The TIP4P potential model,[44] which describes the polar nature of the water molecule efficiently, is best suited for modeling interactions with sodium chloride.[32] Comparisons between various water models show the more advanced TIP5P model performs better at predicting the density of supercooled water, but at temperatures above 273 K, TIP4P comes closest to predicting both measured liquid density[45] and surface tension.[46] Liquid water properties calculated using TIP4P are summarized and compared with their measured values in Table 1.

The model has a charge center with a fixed negative charge placed on the bisector of the HOH angle, with fixed charges on the hydrogen atoms. The internal structure of water is considered to be rigid, with the OH bond lengths constrained at 0.9572 Å, the HOH bond angle at 104.52°, and a separation of 0.15 Å between the oxygen atom and charge center. The form of the

TABLE 1: Comparison between Selected Liquid Water Properties at 300 K and 1 Atm Calculated from the TIP4P Potential and Measurements[a]

	calcd, TIP4P	meas
ρ, g cm^{-3}	1.001	0.997
ΔH_{vap}, kcal mol^{-1}	10.65	10.51
C_P, cal mol^{-1} deg^{-1}	20.0	18.0
D,10^{-5} ms^{-2}	3.30	2.30
σ, mN m^{-1}	61.2	71.7

[a] Surface tensions obtained from Ismail;[46] all other properties from Jorgensen.[45]

TABLE 2: B−H−M Potential Parameters[37] for Na and Cl Used in Eq 4

pair	A/kJ mol^{-1}	ρ/Å	C/kJ mol^{-1}Å^6	D/kJ mol^{-1} Å^8
Na−Na	40 872.1	0.312	101.2	48.2
Cl−Cl	33 628.7	0.318	6981.5	13 429.1
Na−Cl	121 081.4	0.318	674.5	837.1

intermolecular potential is

$$V(r_{ij}) = \frac{e^2 q_i q_j}{r_{ij}} + \epsilon_{ij}\left(\left(\frac{\sigma_{ij}}{r_{ij}}\right)^{12} - \left(\frac{\sigma_{ij}}{r_{ij}}\right)^{6}\right) \quad (5)$$

with ϵ_{ij} and σ_{ij} as LJ-type interaction parameters, and the indices sum over the four force centers in the water molecule.

Ion−water interactions are modeled using LJ-type interactions.[47] The LJ center is placed solely on the oxygen atoms, and there are no LJ-type interactions with either the water hydrogens or the extra charge center present in the TIP4P model. Air is modeled using a 4:1 mixture of nitrogen and oxygen molecules, which also interact using the LJ potential. The amount of water vapor and minor constituents in the air phase are small and not included. Modeling dry, rather than wet, air in contact with the liquid phases will have a negligible effect on interfacial energy at the simulation scale, which is neglected. Parameter values used for potentials in eqs 5 and 6 and their sources are listed in Tables 2 and 3. Cross terms for all LJ interactions are calculated using the Lorentz−Berthelot combination rules, that is, $\epsilon_{ij} = \sqrt{\epsilon_{ii}\epsilon_{jj}}$ and $\sigma_{ij} = (\sigma_{ii} + \sigma_{jj})/2$.

B. Energy Difference Method. In a constant pressure (NPT) ensemble, the appropriate thermodynamic property for calculating the surface tension is the Gibbs free energy,

$$\sigma = \frac{G^{\alpha\beta} - (G^{\alpha} + G^{\beta})}{A} \quad (6)$$

Although the use of eq 6 is thermodynamically rigorous, estimation of surface free energy using simulations is limited for multicomponent phases and by computational resources.[29] A quantity that is readily available for multicomponent mixtures is the enthalpy,

$$H = G + TS \quad (7)$$

From our simulations, the enthalpy H is evaluated as a molar quantity and is an intensive property independent of the number of particles. To obtain the correct free energy difference, we must include the same number of molecules in each simulation. Substituting the relationship between enthalpy and free energy in eq 3, we arrive at

$$\sigma = \frac{H^{\alpha\beta}n^{\alpha\beta} - (H^{\alpha}n^{\alpha} + H^{\beta}n^{\beta})}{A} - T\frac{S^{\alpha\beta}n^{\alpha\beta} - (S^{\alpha}n^{\alpha} + S^{\beta}n^{\beta})}{A} \quad (8)$$

TABLE 3: Lennard-Jones Parameters[47−51] Used in Eq 5

pair	ϵ/kJ mol^{-1}	σ Å
O−O (water)	0.6502	3.166
Na−O	0.5216	2.876
Cl−O	0.5216	3.785
N−N	0.593	3.798
O−O (air)	0.886	3.467
Na−Na	0.418	2.583
Cl−Cl	0.418	4.400

The simulation cells are set up such that the conditions $n^{\alpha\beta} = n^{\alpha} + n^{\beta}$ and $V^{\alpha\beta} = V^{\alpha} + V^{\beta}$ hold, satisfying the requirements of the Gibbs plane of separation.[12] The interfacial area is equal to twice the cross-sectional area of the simulation cell, since two such planes exist in the inhomogenous cell. Note that even in the isothermal−isobaric ensemble, the volume does not change beyond statistical fluctuation, since there is neither a temperature change nor a phase transformation, and the number of molecules is chosen on the basis of the density expected and the cell volume. Since the overall change (rather, fluctuation) in cell volume is minor over the course of a simulation, the plane of separation does not move away from the physical interface. The quantities n and A are both evaluated on a per simulation cell basis, and the products in eq 8 remain pseudo-intensive. If the simulations were repeated using simulation cells twice as large and the same interfacial area, for example, H would remain largely unaffected, with the larger system size reflected in both n^{α} and $n^{\alpha\beta}$, and cancel out. This implies that $H^{\alpha\beta}$ can be split into a contribution from the region close to the interface and the region that behaves like bulk, with a proper simulation set up ensuring that the interface serves as the plane of separation. We can rewrite eq 8 so that a bound on the surface tension is calculated from the energetic terms, with a correction due to the entropic terms; that is,

$$\sigma = \frac{H^{\alpha\beta}n^{\alpha\beta} - (H^{\alpha}n^{\alpha} + H^{\beta}n^{\beta})}{A} - \delta_S \quad (9)$$

where δ_S represents the contribution of the excess surface entropy,

$$\delta_S = T\frac{S^{\alpha\beta}n^{\alpha\beta} - (S^{\alpha}n^{\alpha} + S^{\beta}n^{\beta})}{A} \quad (10)$$

At constant pressure, the excess surface entropy term can be related to the surface tension as[52]

$$\delta_S = -T\frac{\partial\sigma}{\partial T} \quad (11)$$

The surface tension of liquid interfaces decreases with temperature.[53−55] The Guggenheim equation[56] provides an empirical temperature dependence for the available measurements,

$$\sigma = k\left(1 - \frac{T}{T_c}\right)^n \quad (12)$$

where T_c is the critical temperature, n is a critical exponent equal or close to unity, and k is an unknown prefactor. Substituting eq 12 in eq 11, we get

$$\delta_S = nk\left(\frac{T}{T_c}\right)\left(1 - \frac{T}{T_c}\right)^{n-1} \quad (13)$$

indicating that the δ_S term is positive and decreases at subcritical temperatures. Recent phenomenological models suggest that the

TABLE 4: Simulation Cell Edge Lengths, Number of Molecules in Each Cell and Corresponding Density for Bulk Phases Simulated in the Energy Difference Method[a]

bulk phase	cell edge length, Å	N_{mol}	density, kg m^{-3}
NaCl (s)	25.00	348	2147.02
water	25.00	522	998.41
NaCl soln	25.00	580	1355.87
air	745.30	10	1.15

[a] Interfacial cells are constructed by combining one-half of the volume of each bulk cell.

excess surface free energy of crystals forming from the melt is negative along the coexistence curve, due to a reduction in entropy resulting from structural organization in liquid layers in immediate contact with the crystal nucleus.[57−59] In the extreme case in which sufficient liquid ordering occurs, it is possible that δ_S might be negative for the heterogeneous solid−liquid interfaces we have considered, even at concentrations far removed from nucleation conditions. At present, no definitive result is available, and further studies are required. For all solid−liquid and solid−vapor interfaces that show the same trend as liquid−vapor interfaces, δ_S is positive and eq 9 provides an upper bound to the surface tension value. In the specific case of metastable solid crystallization, δ_S has been postulated to be negative, and eq 9 would instead provide a lower bound. For the more general treatment we have used here, we neglect this special case and assume that δ_S is positive for the interfaces in our system so that we can interpret the calculations as an upper bound. The magnitude of δ_S, that is, the extent to which the bound lies above the surface tension, is expected to be relatively small at temperatures away from the critical point, as indicated by eq 13. For solid−liquid and solid−vapor interfaces, we expect the entropic contribution to be small relative to the more important enthalpic contributions to the free energy, indicating that neglecting δ_S will not produce a large error.

The energy difference calculations are carried out at 1 atm for the interfaces of interest. Details of cell edge length and number of simulated molecules are summarized in Table 4 for each bulk phase, and the interfacial phases are constructed by combining cells equivalent to one-half of the volume of the bulk-phase cells. Recent work[60] using Monte Carlo simulations has predicted values slightly lower than the measurements for sodium chloride solubility. Since both the water potential and simulation method are distinct from this work, we use the experimentally determined NaCl solubility to model a saturated solution. Simulations are carried out for a total of 20×10^6 steps, corresponding to a total of 15 ns. The three sets of enthalpy values required to calculate surface tension (between solid NaCl and air) are shown in Figure 1 a as running values. Excluding the initial spin-up period for which statistics are excluded, the simulations show no trend in the mean and are considered to be at equilibrium. Surface tension upper bounds calculated from eq 9 at each time step are shown in Figure 1b. The calculated values retain noise due to the scaling techniques used in the simulation itself. A box-type smoothed line calculated by averaging 55 data points around each individual point indicates no trend in the mean value. The reported value for surface tension upper bound is obtained as an arithmetic mean of the entire data set.

C. Energy Integral Method. The relative magnitude of the entropy correction term in eq 9 can be estimated by comparing our results with a more accurate measure of the surface tension, obtained using the method of Laird and Davidchack,[29] in which the surface energy is evaluated as the reversible work of introducing an interface between two bulk phases in contact. This method is computationally intensive and requires a series of simulations of each phase. As a first step, noninteracting cleaving planes are introduced at an arbitrary position into each bulk phase and then moved to the location of the interface over a series of fixed small displacements. One-half of each bulk phase is then removed by reducing stepwise the electrostatic and Lennard-Jones-type interactions from a relative magnitude of 1 to 0 by modifying the interaction potentials using a multiplicative interaction parameter. The two semiphases are then brought into contact, and the cleaving walls are removed by repeating this process in reverse, that is, by first switching the interaction parameters from 0 to 1 and then moving out the cleaving walls to their initial positions over a series of runs. The net energy difference in following this closed thermodynamic path then provides a measure of the free energy of formation of the interface. The surface energy, w, as defined in eqs 9−13 by Laird and Davidchack[29] can be represented by changing notation as

$$w = \sum_{j=1}^{i=4} \int_{\lambda_{j,i}}^{\lambda_{j,f}} \frac{\partial E_j}{\partial \lambda_j} \, d\lambda_j \tag{14}$$

where λ_j is, in turn, the interaction parameters corresponding to electrostatic and L-J interactions and the z-coordinate of the cleaving wall, with appropriate limits in each case.

This method can be adapted for our system by simulating only single-component phases and replacing the BHM potential for NaCl with a truncated LJ potential.[51] Air is simulated as pure nitrogen for this method. The cleaving walls introduced into each bulk phase consist of molecules of that phase that are frozen in place and have interactions only with the phase across the interface. Electrostatic and Lennard-Jones interactions are removed by reducing ionic charge and LJ well depth, respectively. Hysteresis error due to formation of metastable crystalline structures in the melt phase are negligible in our work, since we only consider a solid NaCl phase. In the stage in which cleaving walls are introduced, we begin each simulation with the molecules at rest. This requires longer equilibration times but reduces the hysteresis error to less than statistical variability. Simulation cell sizes used were as listed in Table 4; however, due to the larger number of runs required, the total simulation length was limited to 4×10^6 time steps, corresponding to 3 ns.

D. Test Area Method. The test area method developed by Gloor[1] and co-workers is an improvement over both the energy difference method, since it directly simulates the surface tension, and the energy integral method, providing a significant reduction in computational costs. The method relies on estimating the perturbation in Helmholtz free energy when a perturbation to the total area of an interface is introduced, keeping all other properties constant. For a system perturbed from a reference state α to a state β, the change in Helmholtz free energy can be expressed in terms of their canonical partition functions as

$$\Delta F_{\alpha \to \beta} = -kT \ln\left(\frac{Q_\beta}{Q_\alpha}\right) \tag{15}$$

For systems containing the same number of molecules of the same species at the same volume and temperature, the ratio of

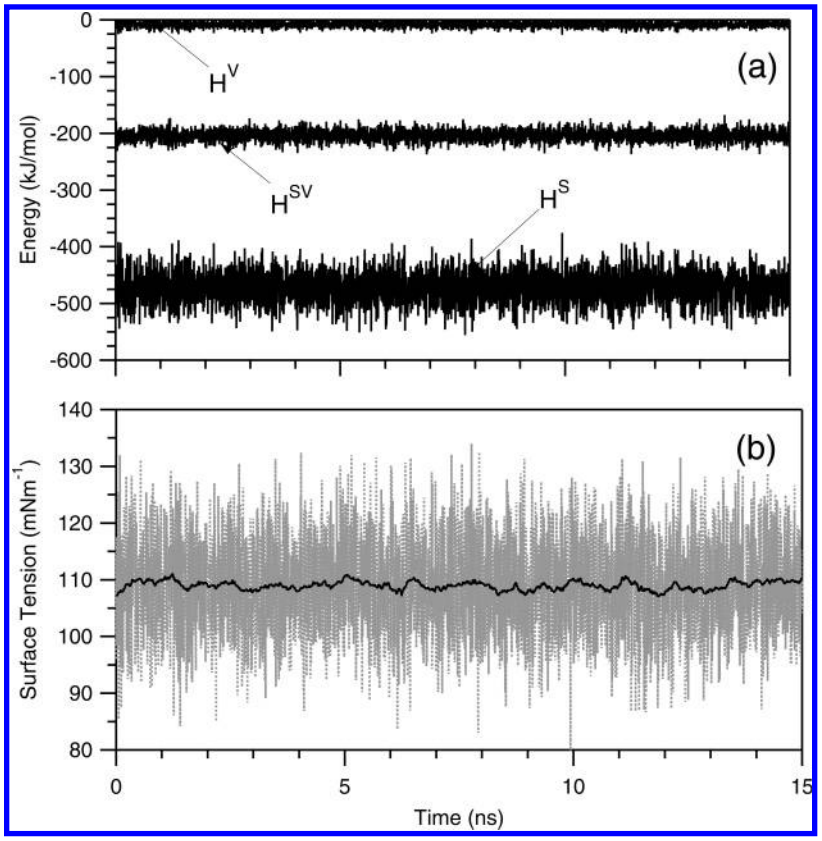

Figure 1. System properties required for calculating surface tension. (a) Total enthalpy for simulation cells containing NaCl solid (s), air (v), and NaCl−air interface (sv). (b) Surface tension calculated using eq 9 along with a trend line from a boxed average.

canonical partition functions is equivalent to the ratio of the configurational integrals,

$$\frac{Q_\beta}{Q_\alpha} = \frac{\int d\mathbf{r}^N \exp(-U_\beta^c/kT)}{\int d\mathbf{r}^N \exp(-U_\alpha^c/kT)} \tag{16}$$

where U^c represents the configurational energy of each molecule with coordinates **r**. Assuming that the configurational energy of the system β is a perturbation to that of the reference state α, the free energy change is proportional to the logarithm of the Boltzmann factor of ΔU averaged over configurations of the reference state.

$$\Delta F_{\alpha\to\beta} = -kT \ln < \exp(-\Delta U^c/kT) > \tag{17}$$

The surface tension for a small change in surface area can be obtained as

$$\sigma = \left(\frac{\partial F}{\partial A}\right)_{NVT} \approx -\frac{kT}{\Delta A}\ln <\exp(-\Delta U^c/kT)> \tag{18}$$

The accuracy of the calculation can be improved by using a center-difference approximation for the expansion of the free energy derivative by introducing equal perturbations of opposite sign to the reference state such that

$$\sigma = \left(\frac{\partial F}{\partial A}\right)_{NVT} \approx -\frac{kT}{2\Delta A}(\ln <\exp(-\Delta U^{c-}/kT)> - \ln <\exp(-\Delta U^{c+}/kT)> \tag{19}$$

Although this algorithm is equally valid for both the Monte Carlo and molecular dynamics frameworks, this work represents the first implementation using MD and possibly the first with specific potentials for systems with available experimental measurements for comparison. Vega and de Miguel[61] calculated the surface tension of water using the test area method with available interaction potentials in a MC framework, obtaining results consistent with earlier calculations. In this work, we implement the algorithm using three interfacial cells constructed with the number of molecules listed in Table 4 having equal volumes but different surface areas such that $A_2 = A_1(1 + 0.0005)$ and $A_3 = A_1(1 - 0.0005)$. The cells are simulated in parallel at NVT conditions for 20×10^6 steps of 0.75 fs each, with the configurational energy recorded after every 5000 steps. Each of these intermediate steps is used to calculate the ensemble average, analogous to the MC ensemble cycles implemented by Gloor et al.[1] The values for $-\Delta U^c$ and $\exp(-\Delta U^c/kT)$ are illustrated in Figure 2 for the NaCl−air interface. Due to the random nature of the fluctuations in magnitude of the configurational energy change, a complete ensemble mean tends to be dominated by extreme outliers, causing a loss of precision. To remove this nonlinear effect of outliers on the results, surface tension is also calculated using a trimmed mean[62] within the 99 and 98 percentile of the ensemble median value. The results are summarized in Table 5. Further reduction in the number of included points to the 97 and 96 percentiles results in a decrease in the surface tension value, but no reduction in standard deviation, indicating that the trimming is excessive. Surface tension was also calculated using the forward difference formula of eq 18, in which only a positive perturbation to the reference state is considered. The use of eq 18 has the advantage of requiring only two parallel simulations but yields surface tensions comparable to those calculated from eq 19 with larger corresponding standard deviations. The savings in computational resources are offset by a loss in precision. Calculations performed using a smaller relative perturbation of $\Delta A = 0.0003A$ also yield results with a larger standard deviation,

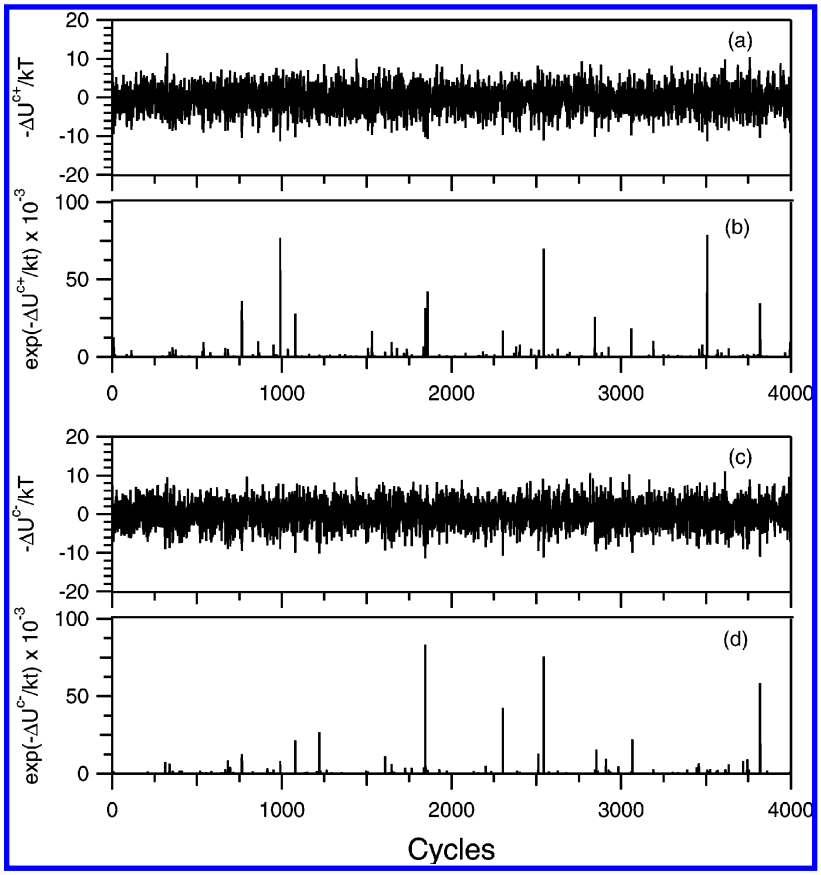

Figure 2. Magnitudes of perturbations in using the test area method described in Section 2D for calculating surface tension of the NaCl−air interface on the basis of the central difference equation. (a, b) Scaled changes in configurational energy and corresponding Boltzmann factor between the reference and positively (increased interfacial area) perturbed states, calculated over 4000 cycles of 5000 steps each. (c, d) Equivalent quantities for the negatively (decreased interfacial area) perturbed state. The averages of these data sets tend to be dominated by the extreme outliers.

TABLE 5: Surface Tension Values Calculated Using Eq 19[a]

interface	σ, mN m^{-1}	σ_{99}, mN m^{-1}	σ_{98}, mN m^{-1}
NaCl-soln	70 ± 23	63 ± 7	59 ± 6
water−air	74 ± 22	65 ± 9	63 ± 8
soln−air	94 ± 27	82 ± 9	81 ± 8
NaCl−air	170 ± 29	117 ± 8	105 ± 8

[a] The averages over the entire ensemble tend to be dominated by extreme outliers, particularly affecting the standard deviation. Surface tensions are also calculated by averaging only points within the 99th and 98th percentile of the median ensemble value, leading to an improvement in both accuracy and precision.

indicating that the perturbation to the reference state might be too small in comparison with the random fluctuations expected in MD. The relative perturbation of ± 0.0005 is used for the calculations to optimize accuracy and precision, consistent with earlier work.[1,61]

III. Results and Discussion

Three different thermodynamic approaches are used to calculate surface tensions in the NaCl−air−water system. The simplest energy difference method is easiest to implement and computationally inexpensive but yields only upper bounds to the surface tension value. The energy integral method yields values that are within 5−15% of the surface tension measurements but is limited by the extensive computation required (more than 10 times the number of computations involved in using eq 9) and the inability to simulate mixed systems (such as saturated air and NaCl solution). The test area approach implemented using MD provides accurate values for surface tension at a relatively low computational cost but is very sensitive to random outlying values in the simulation. This problem can be partly circumvented by excluding extreme outliers. Calculated values for interfaces of interest using each of the three methods are summarized in Table 6. For solid interfaces, the calculated NaCl−air and NaCl−solution surface tensions using each of the methods compare well within the range of errors. Although the contribution of entropy for these interfaces cannot be ignored, the use of eq 9 provides a reasonable first approximation to the rigorous methods; a significant saving in computational cost; and easy generalization to mixed phases, such as solutions.

The calculated mean upper bound for σ^{lv} (lv = liquid/vapor) (water−air) of 73 mN m^{-1} from the energy difference method is closer to the measured surface tensions, which range from 70 to 74 mN m^{-1},[64−67] than either rigorous calculation. This agreement may be an unusual artifact of the fact that we expect to establish an upper bound for the surface tension values with this method and that the TIP4P potential has been shown to underpredict the surface tension for water.[46,61] These opposing effects lead to a value that is close to the measurement for the water−air interface. An estimate of the value of δ_S for water can be obtained by combining eq 13 with temperature-dependent values of surface tension. From the data of Vega[61] for the TIP4P potential, $\delta_S = 23.8$ mN m^{-1} at 300 K. On the basis of the test area method, this yields a value of 89.8 mN m^{-1} which is comparable to the upper bound obtained from the energy difference method. The addition of salt to the liquid phase, replacing water with a saturated solution, raises the value of σ^{lv} (soln−air) to 82 mN m^{-1} which is within the measured range

TABLE 6: Calculated Surface Tensions and Reductions in Uncertainty

interface	σ (expt)	σ^{ED}	σ^{EI}	$\sigma_{99}{}^{TA}$	calcd range	uncertainty reduction, %
NaCl−water		64 ± 4	57 ± 5		52−62	
NaCl−soln	17−187 [63]	59 ± 4		63 ± 7	56−63	96
NaCl−air	100−270 [52]	109 ± 8	114 ± 6	117 ± 8	108−117	95
water−air	70−74 [64−67]	73 ± 6	66 ± 4	65 ± 9	62−70	N/A
soln−air	80−85 [64, 52, 68, 8]	89 ± 4		82 ± 8	74−90	N/A

All magnitudes are reported in mN m^{-1}. Column 3 lists upper bounds calculated using the energy difference (ED) method of eq 9; column 4 lists values calculated using the energy integral (EI) method adapted from Laird and Davidchack.[29] Column 5 lists values calculated using the test area (TA) methods adapted from Gloor et al.[1] using the 99th percentile values listed in Table 5. Measurements where available are included in column 2 for comparison. The combined range of uncertainty from the calculated surface tensions and corresponding upper bounds is listed in column 6. The uncertainty reduction is defined as the relative reduction in the range of surface tension values between reported measurements and calculations in this work.

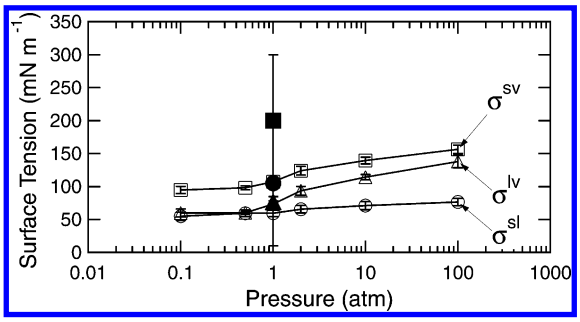

Figure 3. Pressure dependence of surface tension for the NaCl−air−water system. Calculated values with error bars showing estimated uncertainties are shown for the NaCl−air (squares), NaCl−solution (circles), and water−air (triangles) interfaces. Filled symbols are experimental values at 1 atm, as from Table 6.

of 80−85 mN m^{-1},[8,52,64,68] but it is of limited value, since liquid surface tensions can be measured with a higher precision (±1%) than the statistical error associated with the calculation. Furthermore, as estimated, the entropic contribution to liquid−vapor surface tension is non-negligible. The value of this work lies in that the calculated values for surface tensions of the solid interfaces have considerably less uncertainty (due to both the entropy approximation and the statistical variability) than the large experimental uncertainties. The calculated values and upper bounds for σ^{sv} (sv = solid/vapor) of 109, 114, and 121 mN m^{-1} and for σ^{sl} (sl = solid/liquid) (NaCl−soln) of 59 and 63 mN m^{-1} all fall within reported experimental uncertainty and reduce the possible range of values by an order of magnitude. For the solid−vapor interface, the reported experimental range of 100−270 mN m^{-1} [52] is reduced to 108−117 mNm^{-1}. For the solid−solution interface, the reduction in uncertainty is also very valuable, changing the experimental range of 17−187[63] to 57−63 mN m^{-1}.

IV. Pressure Sensitivity

The pressure dependence of surface tension is poorly understood and is studied here for the NaCl−soln, NaCl−air, and water−air interfaces at pressures ranging from 0.1 to 100 atm. Figure 3 shows the upper bounds for surface tensions with the energy difference method at six different pressures, with experimentally determined values at 1 atm included for comparison. Each of the interfaces studied shows a positive correlation between pressure and the calculated upper bound for surface tension, with a stronger dependence above 1 atm. There is less than an order of magnitude of expected variation in surface tension over 4 orders of magnitude of pressure.

V. Conclusions

This work reports surface tensions in the NaCl−water−air systems calculated using classical MD simulations by three thermodynamic routes at 300 K and a range of pressures. Calculations based on differences between simulated energies of homogeneous and interfacial systems provide an upper bound for substances that have decreased surface tension with increased temperature. The energy difference method provides upper bounds for water−air and soln−air, σ^{lv}, which are within ±6 mN m^{-1}, or 7% of experimental measurements. The calculated upper bounds for solid interfaces provide lower uncertainty (±10 mN m^{-1}) than the current range of experimental results from indirect methods for σ^{sv} and σ^{sl} (which have experimental uncertainties of the order of 100 mNm^{-1}, respectively). The energy integral and test area methods provide accurate values for the actual surface tension at high computational cost and lower precision, respectively. The simulated surface tensions of liquid interfaces for σ^{lv} of 66 ± 4 mN m^{-1} (water−air) and 82 ± 8 mN m^{-1} (soln−air) underpredict as compared to measurements, and solid surface tensions for σ^{sl} of 63 ± 7 mN m^{-1} and for σ^{sv} of 117 ± 8 mN m^{-1} provide a significant improvement in the estimated error while remaining within the range inferred from laboratory studies. The simulated surface tension has a weak, positive dependence on pressure for NaCl−air, water−air, and NaCl−soln.

Although novel experimental techniques are needed to quantitatively evaluate solid surface tensions, the reduction in the uncertainty of σ^{sl} significantly improves our ability to predict the behavior of salt surfaces for many applications. For example, the size dependence of deliquescence relative humidity is reduced from 1.08 to 1.04 at 20 nm (as shown by comparing the previous value of $\sigma^{sl} = 29$ mN m^{-1} in curve 5 and the new estimated σ^{sl} of 63, as approximated in curve 7, both in Figure 3 of ref 5). This 5% reduction in the size dependence of deliquescence relative humidity is small but provides results that are more consistent with recent experiments.[69]

Acknowledgment. We thank Brian B. Laird, Gerald Wilemski, Scot T. Martin, Peter R. Buseck, George Biskos, Matthew Wise, and three anonymous reviewers for their suggestions. This material is based upon work supported by the National Science Foundation under Grant no. 0304213. Any opinions, findings, and conclusions and recommendations are those of the authors and do not necessarily reflect the views of the National Science Foundation.

References and Notes

(1) Gloor, G. J.; Jackson, G.; Blas, F. J.; de Miguel, E. *J. Chem. Phys.* **2005**, *123*, 134703.

(2) Martin, S. T. *Chem. Rev.* **2000**, *100*, 3403.

(3) Finlayson-Pitts, B. J.; Hemminger, J. C. *J. Phys. Chem. A* **2000**, *104*, 11463.

(4) Hoffman, R. C.; Kaleuati, M. A.; Finlayson-Pitts, B. J. *J. Phys. Chem. A* **2003**, *107*, 7818.

(5) Russell, L. M.; Ming, Y. *J. Chem. Phys.* **2002**, *116*, 311.

(6) Vaknin, D.; Dahlke, S.; Travesset, A.; Nizri, G.; Magdassi, S. *Phys. Rev. Lett*. **2004**, *93*, 218302.
(7) Heslot, F.; Cazabat, A. M.; Levinson, P.; Fraysse, N. *Phys. Rev. Lett*. **1990**, *65*, 599.
(8) Wu, W.; Nancollas, G. H. *Adv. Coll. Interface Sci*. **1999**, *79*, 229.
(9) Harbury, L. *J. Phys. Chem.* **1946**, *50*, 190.
(10) Hiemenz, P. C. *Principles of Colloid and Surface Chemistry*; Dekker Inc.: New York, 1986.
(11) Prisciandaro, M.; Lancia, A.; Musmarra, D. *AIChE J*. **2001**, *47*, 929.
(12) Rowlinson, J. S.; Widom, B. *Molecular Theory of Capillarity*; Clarendon: Oxford, 1982.
(13) Nicholson, D.; Parsonage, N. G. *Computer Simulation and Statistical Mechanics of Adsorption*; Academic: New York, 1982.
(14) Matsumoto, M.; Kataoka, Y. *J. Chem. Phys.* **1987**, *88*, 3233.
(15) Alejandre, J.; Tildesley, D. J.; Chapela, G. A. *J. Chem. Phys.* **1995**, *102*, 4574.
(16) Zykova-Timan, T.; Ceresoli, D.; Tartaglino, U.; Tosatti, E. *Phys. Rev. Lett*. **2005**, *94*, 176105.
(17) Ohtaki, H.; Radnal, T. *Chem. Rev.* **1993**, *93*, 1157.
(18) Lyubartsev, A. P.; Laaksonen, A. *J. Phys. Chem.* **1996**, *100*, 16410.
(19) Koneshan, S.; Rasaiah, J. C. *J. Chem. Phys.* **2000**, *113*, 8125.
(20) Jungwirth, P.; Tobias, D. J. *J. Phys. Chem. B* **2001**, *105*, 10468.
(21) Lisal, M.; Smith, W. R.; Kolafa, J. *J. Phys. Chem. B* **2005**, *109*, 12956.
(22) Perera, L.; Berkowitz, M. L. *J. Chem. Phys.* **1991**, *95*, 1954.
(23) Jungwirth, P.; Tobias, D. J. *J. Phys. Chem. A* **2002**, *106*, 379.
(24) Shinto, H.; Sakakibara, T.; Higashitani, K. *J. Phys. Chem. B* **1998**, *102*, 1974.
(25) Shinto, H.; Sakakibara, T.; Higashitani, K. *J. Chem. Eng. Jpn.* **1998**, *31*, 771.
(26) Oyen, E.; Hentschke, R. *Langmuir* **2002**, *18*, 547.
(27) Hoyt, J. J.; Asta, M.; Karma, A. *Phys. Rev. Lett*. **2001**, *86*, 5530.
(28) Gonzalez-Melchor, M.; Alejandre, J.; Bresme, F. *Phys. Rev. Lett*. **2003**, *90*, 135506.
(29) Laird, B. B.; Davidchack, R. L. *J. Phys. Chem. B* **2005**, *109*, 17802.
(30) Trokhymchuk, A.; Alejandre, J. *J. Chem. Phys.* **1999**, *111*, 8510.
(31) Binder, K. *J. Phys. Chem. A* **1982**, *25*, 1699.
(32) Bahadur, R.; Russell, L. M.; Alavi, S.; Martin, S. T.; Buseck, P. R. *J. Chem. Phys.* **2006**, *124*, 154713.
(33) Forester, T. R., Smith, W., Eds. *DLPOLY 2.14;* CCLRC, 1995.
(34) Nose, S. *J. Chem. Phys.* **1984**, *81*, 511.
(35) Nose, S. *Mol. Phys.* **1984**, *52*, 255.
(36) Hoover, W. G. *Phys. Rev. A: At., Mol., Opt. Phys.* **1985**, *31*, 1695.
(37) Frenkel, D.; Smit, B. *Understanding Molecular Simulation*; Academic: New York, 2000.
(38) Allen, M. P.; Tildesley, D. J. *Computer Simulation of Liquids*; Oxford University Press: New York, 1987.
(39) Rappaport, D. C. *The Art of Molecular Dynamics Simulations*; Cambridge University Press: New York, 1987.
(40) Gibson, K. D.; Scheraga, H. A. *J. Phys. Chem.* **1995**, *99*, 3752.
(41) Huggins, L.; Mayer, J. E. *J. Chem. Phys.* **1933**, *1*, 643.
(42) Gruenhut, S.; MacFarlane, D. R. *J. Non-Cryst. Solids* **1995**, *184*, 356.
(43) Bhatt, D.; Chee, R.; Newman, J.; Radke, C. J. *Curr. Opin. Colloid Interface Sci*. **2004**, *9*, 145.
(44) Jorgensen, W. L.; Chandrasekhar, J.; Madura, J. D.; Impey, R. W.; Klein, M. L. *J. Chem. Phys.* **1983**, *79*, 926.
(45) Jorgensen, W. L.; Tirado-Rives, J. *Proc. Natl. Acad. Sci*. **2005**, *102*, 6665.
(46) Ismail, A. E.; Grest, G. S.; Stevens, M. J. *J. Chem. Phys.* **2006**, *125*, 014702.
(47) Smith, D. E.; Dang, L. X. *J. Chem. Phys.* **1994**, *100*, 3757.
(48) Lynden-Bell, R. M.; Rasaiah, J. C. *J. Chem. Phys.* **1997**, *107*, 1981.
(49) Bojan, M. J.; Steele, W. A. *Langmuir* **1987**, *3*, 1123.
(50) Kaneko, K.; Cracknell, R. F.; Nicholson, D. *Langmuir* **1994**, 10, 4606.
(51) Koneshan, S.; Rasaiah, J. C.; Lynden-Bell, R. M.; Lee, S. H. *J. Phys. Chem. B* **1998**, *102*, 4193.
(52) Adamson, A. W. *Physical Chemistry of Surfaces*; Wiley: New York, 1990.
(53) Kayser, W. V. *J. Colloid Interface Sci.* **1976**, *56*, 622.
(54) Escobedo, J.; Mansoori, G. A. *AIChE J*. **1996**, *42*, 1425.
(55) Halas, S.; Durakiewicz, T. *J. Phys.: Condens. Matter* **2002**, *14*, l735.
(56) Guggenheim, E. A. *J. Chem. Phys.* **1945**, *13*, 253.
(57) Spaepen, F. *Solid State Phys.* **1994**, *47*, 1.
(58) Wu, D. T.; Granasy, L.; Spaepen, F. *MRS Bull*. **2004**, *29*, 945.
(59) Asta, M.; Spaepen, F.; van der Veen, J. F. *MRS Bull.* **2004**, 29, 920.
(60) Sanz, E.; Vega, C. *J. Chem. Phys.* **2007**, *126*, 014507.
(61) Vega, C.; de Miguel, E. *J. Chem. Phys.* **2007**, *126*, 154707.
(62) Huber, P. J. *Robust Statistics*; Widom: New York, 1981.
(63) Wang, Z. L.; Petroski, J. M.; Green, T. C.; El-Sayed, M. A. *J. Phys. Chem. B* **1998**, *102*, 6145.
(64) Heller, W.; Cheng, M. H.; Greene, B. W. *J. Colloid Interface. Sci*. **1966**, *22*, 179.
(65) Gaonkar, A. G.; Neuman, R. D. *Colloids Surf.* **1987**, *27*, 1.
(66) Jasper, J. J. *J. Phys. Chem. Ref. Data* **1972**, *1*, 841.
(67) Fujii, H.; Matsumoto, T.; Ueda, T.; Nogi, K. *J. Mater. Sci*. **2005**, *40*, 2161.
(68) Abramzon, A. A.; Gauberk, R. D. *Zh. Prikl. Khim.* **1993**, *66*, 1428.
(69) Biskos, G.; Malinowski, A.; Russell, L. M.; Buseck, P. R.; Martin, S. T. *Aerosol Sci. Technol.* **2006**, *40*, 1.